Environ. Sci. Technol. **1999**, *33,* 2758−2764

Separation of an Anionic Surfactant by Nanofiltration

ANTÓNIO C. ARCHER,[†,‡] ADÉLIO M. MENDES,[*,‡] AND RUI A. R. BOAVENTURA[†]

Chemical Engineering Department, Faculty of Engineering, University of Porto, Rua dos Bragas, 4099 Porto Codex, Portugal

The separation by nanofiltration of an anionic surfactant belonging to the alkyl-polyether-sulfate family (critical micellar concentration, cmc = 300 mg/L) was studied. Different asymmetric membranes were tested first, but the assessment of the separations efficiency led to the selection of a strong hydrophilic nanofiltration membrane, negatively charged, with an active layer made of a proprietary polymer. Further experiments were made with this membrane, at various feed surfactant concentrations (up to 20 × cmc), temperatures, and cross-flow velocities. The results revealed a complex behavior, mainly for the permeate flux, showing that the separation depends much on the physical-chemical properties of the surfactant and the electrostatic interactions between the membrane and the ionic species in the aqueous solution. To explain the changes of the permeate flux with the feed surfactant concentration, namely the flux increase in the micellar critic region, a mechanism based on physical-chemical interactions between the membrane and the surfactant is proposed. Because of the high values obtained for the permeate flux and rejection (maximum of 204 L/(m^2·h) and 99.5%, respectively), environmental applications of the process appear to be interesting, specially in the pretreatment of industrial effluents with a significant amount of anionic surfactants.

Introduction

Surfactants find many applications in domestic as well as in industrial product formulations. They are used mainly as cleaning agents, and so they are rejected together with large volumes of domestic or industrial wastewaters. When released in the natural water bodies, they cause a negative impact, and their presence in the effluents strongly reduces the performance of biological wastewater treatment plants (*1*). In Portugal, as in many other countries, environmental legislation imposes concentration limits (2 mg/L) for anionic surfactants to be discharged directly into streams or spread on the ground.

Membrane separation technology has been finding more and more applications in the environmental area (*2*) namely in wastewater treatment (*3*). Surfactant separation by membrane processes can be used for instance inside the industrial plant, with the objective of recycling most of surfactant, or at the wastewater treatment plant as a pretreatment process or a polishing step before the effluent discharge. The micellar-enhanced ultrafiltration (MEUF) is also a very recent process that can be used for removing dissolved organics or multivalent ions from aqueous streams (*4, 17*). The separation is enhanced by adding to the aqueous stream a surfactant that is later removed as micelles containing the pollutants. This new process is based on the high capacity of micelles to solubilize organic compounds and metal ions and can be compared with other sorbent based processes, like those using activated carbon. An appropriate concentration of surfactant is added to a stream containing organic pollutants or metal ions, so that a large fraction of the surfactant exists in the micellar form. The organic molecules diffuse into the micelles and stay there due to (the) their high solubilization capacity (*9, 10, 17*). When the resulting solution is passed through an ultrafiltration membrane having pore diameters smaller than the micelle diameter, most of the surfactant and the organic solute remain in micelles in the retentate solution. A calculation procedure for design MEUF units to separate organic pollutants from water streams was developed by Markels et al. (*17*).

The surfactant micelles have a high electrical potential that can cause the multivalent ions to bind or sorb on the micelles due to electrostatic attraction. The emulsion can then be treated by ultrafiltration and micelles rejected by large-pore membranes. Rejections of 99.8% have been observed for divalent metal ions with large membrane pore sizes and high flux (*4*). This new process has proved to be interesting for cleaning watewaters from printing circuit, metal surfaces plating and photographic industries, and refineries. It has also been used to remove nitrates from sanitary landfill leachates (*11*).

The first membrane process used to separate surfactants was ultrafiltration, at the beginning of the 1970s decade (*5*). Later on, to increase the reverse osmosis performance in desalination systems, a surfactant was added to seawater. The surfactant was adsorbed at the membrane surface, thus creating a secondary membrane. Ultrafiltration is also being used to concentrate emulsions (*6*). The dynamics and the steady-state behavior in a cross-flow microfiltration process of a cationic surfactant were evaluated by Akay and Wakeman (*7, 8*). Markels et al. (*16*) studied the micellar surfactant cross-flow ultrafiltration. These authors developed a model considering both the surfactant fouling effect and the intrinsic membrane resistance. Markels et al. (*15*) also studied the mass transfer of surfactants across ultrafiltration membranes. These researchers succeeded to determine the intrinsic rejection coefficients for surfactant monomer and micelle. The intrinsic rejection coefficients are important parameters on modeling surfactants ultrafiltration separations.

In steady-state ultrafiltration, permeate flux decreases when increasing surfactant concentration, down to a minimum corresponding to the formation of a gel layer, which corresponds to a bulk concentration known as gel concentration (c_g) (*12*). This concentration seems to be independent of the membrane pore size and cross-flow. The gel concentration is much higher than the critical micellar concentration (cmc), usually 200−500 times higher, and seems to be related to the formation of stable viscous phases (hexagonal and cubic). When the membrane molecular weight cutoff is close to 1000 amu (the upper cutoff limit of nanofiltration), it was noticed (*13*) that the steady-state permeate flux increases when increasing feed concentration and then level-off up to 50 × cmc. Laslop and Staude, cited by Akay and Wakeman (*12*), found that fouling occurs at lower feed concentration for hydrophilic membranes, since the surfactant also forms

* Corresponding author phone: 351-2-2041695; fax: 351-2-2000808; e-mail: mendes@feup.pt.

† LSRE—Laboratory of Separation and Reaction Engineering.

‡ LEPÆ—Laboratory of Process, Environment and Energy Engineering.

10.1021/es980737c CCC: $18.00
Published on Web 07/03/1999

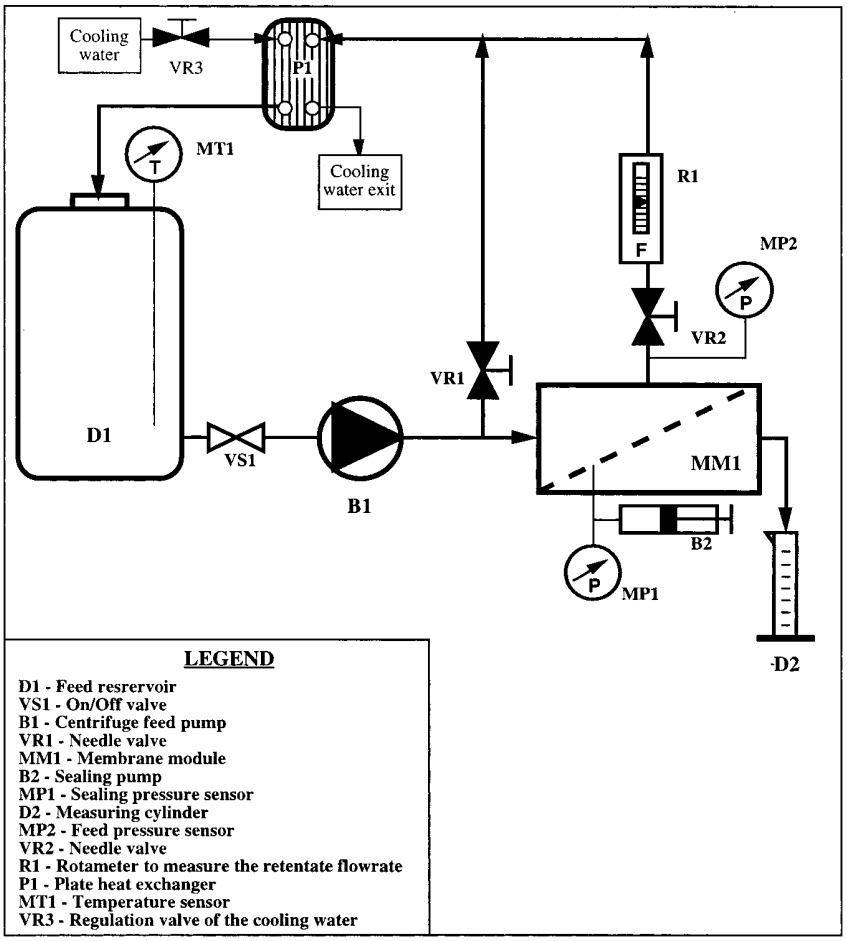

FIGURE 1. Sketch of the experimental setup.

crystal or solid phase at lower concentrations.

The presence of electrolytes, specially polyvalent electrolytes, strongly affects the physicochemical properties of the ionic surfactants. The electrolytes reduce the electrostatic repulsion among the surfactant heads, allowing micelles to form at lower concentrations and so reducing the cmc. The association between micelles and polyvalent ions is just the MEUF separation basis (*4*). For nonionic surfactant solutions, presence of the electrolyte has no effect on the separation.

The objective of this work was to produce useful results to develop a membrane technology for (i) removing surfactants from wastewaters, (ii) recycling surfactants inside an industrial plant, or (iii) recovering them in micellar enhanced processes. Nanofiltration was the selected separation process as it has been the less studied process and referred to adequately separate molecules and ions with a molecular mass up to 500 g/mol (*14*). On the other hand, despite ultrafiltration being used to separate surfactants it is not efficient enough to reach the maximum surfactant discharge limits imposed by law (*15*). After selecting the most efficient membrane, several nanofiltration membranes, with different molecular weight cutoffs and water affinities, will be tested to separate an anionic surfactant from an aqueous stream.

Experimental Section

Experimental Setup. The basic unit of the nanofiltration laboratory setup used in the experimental work is sketched in Figure 1. It is a planar membrane module from Osmonics − U.S.A. (SEPA CF Membrane Cell), with 155 cm^2 useful membrane area. At the module inlet, a fraction of the flow is recycled through a plate heat exchanger (ARSOPI − Portugal, model FH00-MJ-12, with 0.11 m^2 transfer area) and the other fraction fed to the membrane module. The retentate flowrate is measured by a rotameter (R1) and its pressure is followed up by a pressure sensor (MP2). The retentate stream is also recycled to the reservoir through the plate heat exchanger. It is possible with this arrangement to independently control the feed flowrate and pressure. The reservoir was chosen to have such a volume that it was possible to consider the feed composition constant in the course of each experiment. The membrane module also includes a high foulant spacer in the retentate side. Osmonics proposes the following relationship for the cross-flow velocity over the membrane:

$$u\ (\mathrm{m/s}) = 0.11 \times Q\ (\mathrm{L/min}) \qquad (1)$$

The pump used is a multistage centrifugal pump, TONKO-FLO, Model SS526X, from Osmonics. It delivers a maximum flowrate of 4.2 L/min at 15 bar.

The feed pressure and the retentate flowrate were adjusted by tuning needle valves VR1 and VR2 (Figure 1). The temperature was controlled by adjusting the cooling water flowrate (needle valve VR3), and the permeate flowrate was measured using a 100 mL graduate cylinder and a stopwatch.

The first experiment was designed to identify the most promising nanofiltration membrane, from the available set (Table 1). Then, several runs were performed with the selected membrane to study the membrane permeability and rejection as a function of the cross-flow velocity, retentate pressure, surfactant concentration, and temperature.

TABLE 1. Characteristics of the Experimented Nanofiltration Membranes (SEPA Series, OSMONICS)

membrane reference	selective layer	surface charge/ water affinity	MWCO (amu)	NaCl rejection (%)	recommended pressure/max. pressure (bar)	pH range	max. temp (°C)
HG 19	polysulfone	hydrophobic	1000−5000	0	7/27	1−13	100
SP 12	cellulosic polymer	slightly hydrophobic	600−800	1−10	14/20	2−8	50
SV 10	cellulosic polymer	hydrophilic	500−600	30−50	14/27	2−8	50
SX 01	cellulosic polymer	hydrophilic	400−500	50−70	14/34	2−8	50
SX 10	cellulosic polymer	hydrophilic	400−500	50−70	14/34	2−8	50
MX 07	polyamide	neutral	300−500	50−70	7/69	2−12	80
BQ 01	made not available by OSMONICS	strongly hydrophilic/ negative surface charge	200−300 (obtained for polar molecules)	30−50	14/69	3−10	100

TABLE 2. NEOPON LOS 2 N 70 Technical Characteristics

class	anionic surfactant
type	sodium lauryl-ether-sulfate, natural alcohol cut
number CAS	1335-72-4
average molecular mass (g/mol)	385
active matter, 385 g/mol (% by weigh)	70 ± 2 (69.5%)
free oil (% by weigh)	<3
sodium sulfate (% by weigh)	<1 (0.36%)
sodium chloride (% by weigh)	<0.1 (0.02%)
pH (10% diluted in water)	7−8 (7.75)
density (g/cm^3)	1.09
biodegradability (NFT 73 260)	>98%
main uses	shampoo formulations and bath foam (usual concn: 13−15%)

Nanofiltration Membranes. A set of seven nanofiltration membranes from Osmonics (SEPA series) were tested. Some membrane characteristics as the selective layer material, molecular weight cutoff, and hydrophobicity are listed in Table 1 together with other data.

Anionic Surfactant. Among all possible surfactants it was first decided to select one from the anionic group, as this is the most relevant one for both industrial and domestic uses. The alkyl-polyether-sulfate ionic surfactant class presents low toxicity, high water solubility, and resistance to electrolytes. This class of surfactants also shows an excellent chemical stability, necessary for MEUF processes. So, the selected surfactant was the sodium lauryl-ether-sulfate C_{12} natural cut (NEOPON LOS 2 N 70, by WITCO) with 385 g/mol average molecular mass. The chemical formula corresponding to the C_{12} alkyl group is

$$CH_3(CH_2)_{10}CH_2O(CH_2CH_2O)_2SO_3^-Na^+ \qquad (2)$$

Other properties of the sodium lauryl-ether-sulfate C_{12} natural cut are presented in Table 2.

The cmc of this surfactant is 300 mg/L at 20 °C and does not change significantly in the range of 10−40 °C. The surface tension is 30.7 mN/m at cmc and 20 °C. The phase diagram is not available, but it should be expected that from the cmc up to concentrations of 20−30% (w/w) only monomeric surfactant, spherical, and cylindrical micelles are present (*18*).

For each experiment, a 10 L surfactant solution was prepared, and the concentration was checked by analytical determination.

Chemical Analysis. The surfactant concentration was determined by a simplified version of the MBAS method, described in *Standard Methods for the Examination of Water and Wastewater* (*19*). The simplifications are justified by the diluted solutions of a single component used in this work.

TABLE 3. Experimental Results for the Nanofiltration Membranes[a]

membrane reference	no. expt	T (°C)	P (bar)	Q_a (L/h)	c_0 (mg/L)	J_∞ (L/ m^2/h)	c_p (mg/L)	I (%)
HG 19	2.0	24	7	360	155.1	20.4	41.0	73.6
HG 19	2.1	24	7	120	155.1	16.8		
HG 19	2.2	24	15	180	155.1	52.8		
HG 19	2.3	24	4	360	155.1	16.8		
SP 12	9	14	14	360	202.8	4.2	42.4	79.1
SV 10	6	21	14	360	208.5	33.6	18.3	91.2
SX 01	3	22	12	360	197.5	18.6	33.8	82.9
SX 10	4	21	14	360	216.8	33.0	13.6	93.7
MX 07	5	22	12	360	216.8	29.4	2.1	99.0
MX 07	7	20	14	360	104.3	48.0		
BQ 01	8	14	14	360	224.3	67.8	5.0	97.8

[a] Symbols: T, temperature; P, feed pressure (relative); Q_a, feed flowrate; c_0, feed concentration; J_∞, steady-state permeate flux; c_p, permeate concentration; and I, rejection.

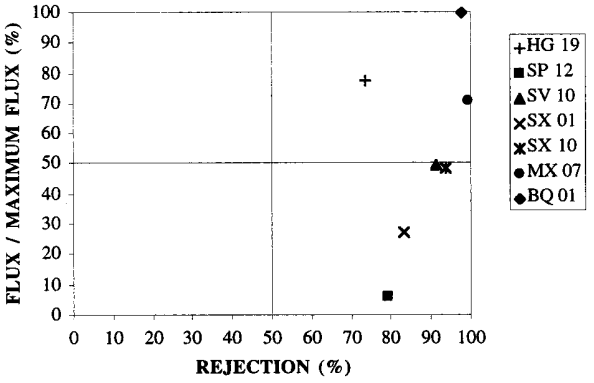

FIGURE 2. Diagram for selecting the more efficient membrane.

Results and Discussion

The results of the first experiments are summarized in Table 3, sorted by the membrane MWCO in ascending order. A first run (no. 1) was performed to test the experimental setup and evaluate the heat exchange needs. All the experiments were performed at a surfactant feed concentration of 300 mg/L, below the cmc, and most of them at around 20−24 °C. It was aimed to choose the membrane with the highest permeate flowrate and rejection. From Figure 2, built up from data of Table 3, it is apparent that the most promising membrane is BQ 01, even considering that experiment no. 9 was performed at a lower temperature (14 °C).

The BQ01 membrane selective layer is a right protected polymer whose composition was not made available by Osmonics. The only information supplied was that the

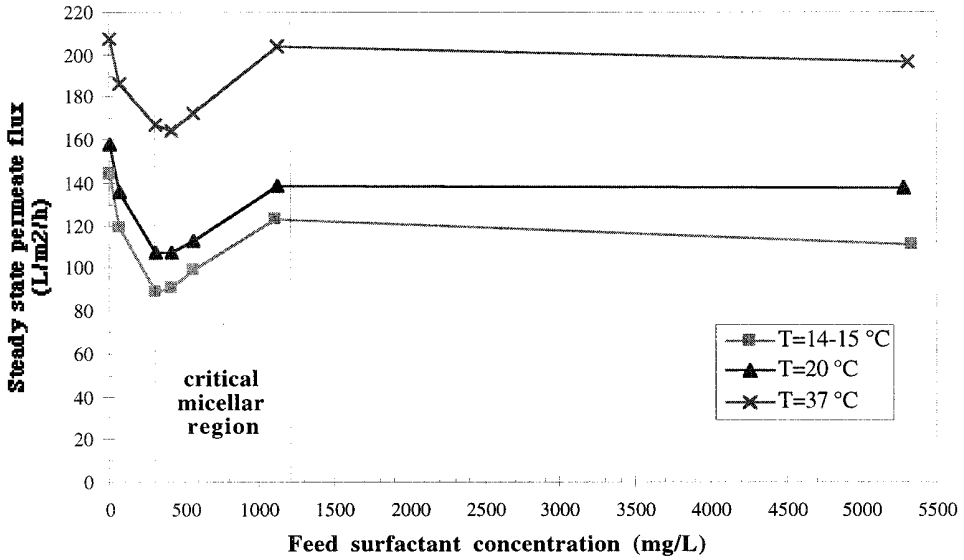

FIGURE 3. Steady-state permeate flux versus feed concentration for three different temperatures and 0.7 m/s cross-flow velocity.

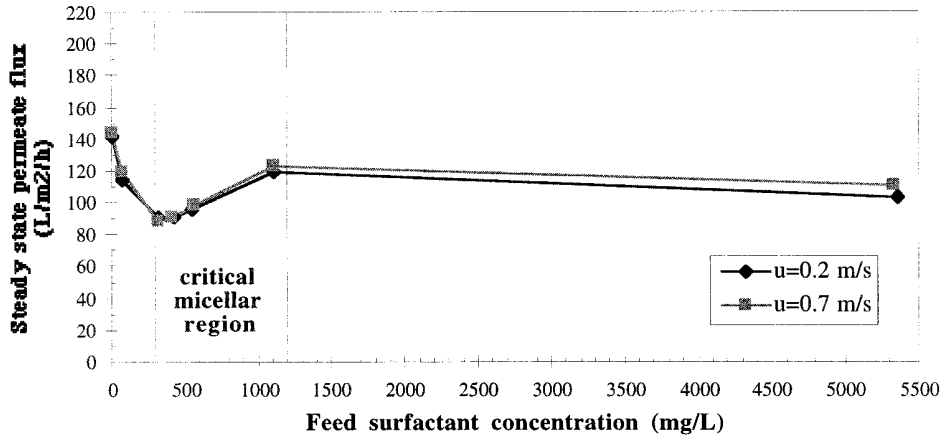

FIGURE 4. Steady-state permeate flux versus feed concentration for two different cross-flow velocities, at 14 °C.

membrane has between 200 and 300 MWCO and is negatively charged (Table 1).

The results in Table 3 show that the permeate flux is not related to the MWCO, since the membranes with smaller pores (MX 07 and BQ 01) show a higher flux. The experiments performed with membrane HG 19 (nos. 2, 2.1, 2.2, and 2.3) show that the permeate flux is more sensible to the pressure gradient than to the feed composition. This indicates a small polarization resistance in this system.

From these results it is also apparent, with some exceptions, that the rejection increases as MWCO decreases. Membrane SV 10, that has a selective layer similar to that of membrane SX 01, a hydrophilic cellulose polymer, shows a higher rejection than the former one. So, the membrane chemical nature has a determinant effect on the rejection.

The flowrate decay at the beginning of the separation is very fast, and the steady state is reached after 2−3 min, with a standard deviation of 4%.

Using the selected BQ 01 membrane several new experiments were performed at the maximum recommended feed pressure, 14 bar. The experiments were performed at two different feed fluxes, three different temperatures, and several feed concentrations. The results are summarized in Figures 3 and 4.

From Figure 3 it is apparent that the pattern of the permeate flux defines three different regions. In the first region the permeate flux rapidly decreases with the feed concentration, until a minimum value close to the critical micellar concentration. The second region, named critical micellar region, starts at that point and goes on until the permeate flux attains its maximum value, close to the pure water flux. Finally, the third region is characterized by a slow permeate flux decreasing.

In the first region, the concentration polarization or surface sorption effect should prevail, thus explaining the rapid permeate flux decreasing with the feed concentration. The surface tension decreases with the surfactant concentration until a minimum is reached at cmc. This allows a better contact between membrane and solution, which, given the fact the membrane surface is negatively charged, also promotes the dissociated anionic surfactant concentration to rise at membrane surface.

The second region starts at 300 mg/L (cmc) surfactant feed concentration and goes up to 1200 mg/L. In this region the micelles are formed and developed, and the dynamic resistance to the permeate flux decreases with the feed concentration. It is proposed the following mechanism to explain the permeate flux resistance decreasing (1) at cmc, the first spherical micelles form close to the membrane surface, where the surfactant concentration is higher, and (2) in a second moment these micelles start moving over the membrane surface, due to the tangential feed flux, incorporating more free surfactant molecules. The concentration

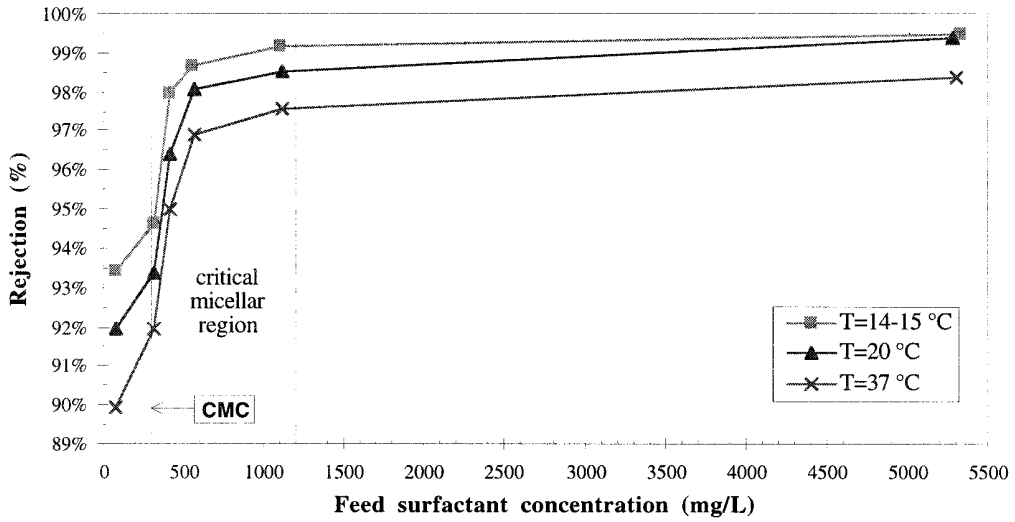

FIGURE 5. Rejection as a function of the feed surfactant concentration for three temperatures, 14, 20, and 37 °C, for a cross-flow velocity of 0.7 m/s.

polarization film is this way continuously destroyed along with the less sorbed molecules.

The surfactant free molecules concentration continuously decreases at the membrane surface, and a very permeable micellar layer takes place. Therefore, at the end of this stage the permeability of the membrane becomes very close to the pure water permeability.

In the third stage the permeate flux starts decreasing slowly. The micelles are already completely formed, most of them forming large spheres and few of them cylinders. The viscosity increases and the micelles packed over the membrane surface, slowly increase the permeate flow resistance. For very high surfactant concentration, and depending on its phase diagram, the hexagonal and then the lamellar phases appear further increasing the permeate resistance and causing a gel layer to form. A nice discussion on the mechanisms of rejection and permeate flux for micro- and ultrafiltration of a cationic surfactant, forming lamella particles, is available in ref *8*.

In Figure 3 it is shown the permeate flux as a function of the feed concentration, for three different temperatures: 14, 20, and 37 °C. It is apparent the permeate flux increases with temperature, while the three curves present the same shape. This means the qualitative reasons for the curves behavior should be the same, since the cmc is almost the same for the three temperatures. The permeate flux should increase with temperature due to the viscosity exponential decreasing (*20*). The permeate flux at the end of the second region recovers to approximately the pure water permeate flux. Meanwhile, this recovery is higher for higher temperatures. This could indicate a more efficient destruction of the polarization concentration film and the removal of the less sorbed molecules, due probably to a easier micelles movement over the membrane surface, according to the proposed model.

In Figure 4 it is shown the permeate flux as a function of the feed concentration for two different tangential surface velocities: 0.2 and 0.7 m/s at 14 °C. It can be seen that, despite the small increase at the end of the critical micellar region and after it, the cross-flow velocity has a weak influence on the permeate flux, for the tested conditions range. This means the concentration polarization effect is small. The spacer used over the membrane should produce enough turbulence to guarantee a low polarization level. At the end of the critical micellar region and after it, the controlling effect on the membrane permeability should be related to the micelles movement over its surface. For higher tangential velocities, the movement of the micelles should increase, producing an efficient erosion of the stagnant film of surfactant free molecules.

For the feed pressure, concentration, and temperature conditions, there is not gel formation or fouling, by liquid crystals deposition on the membrane surface and pores (*6*).

The temperature and tangential velocity effects on the permeate flux described before are in qualitative agreement with the model presented by Grieves et al. (*5*) and referred to by Akay and Wakeman (*12*) for the ultrafiltration of an anionic surfactant.

In Figure 5 is shown the surfactant rejection as a function of the feed concentration for the three temperatures tested: 14, 20, and 37 °C and 0.7 m/s cross-flow velocity.

Here also it is possible to identify three regions of behavior. In the first region, that goes up to the cmc, the rejection seems to be due to Donnan exclusion effect, since the surfactant molecules are essentially dissociated and the organic anion is smaller that the membrane average pore diameter. In the critical micellar region, the rejection rapidly increases due to the micelles formation. These micelles are bigger than the pore diameter and the rejection occurs mainly by a sieving mechanism. The third region is characterized by the level out of the rejection, at values higher than 99%. In this region, the micelles movement should create an effective barrier to the free surfactant molecules, maintaining this way the rejection level very high.

The temperature increase causes the rejection to decrease but does not affect the characteristic behavior of the rejection as a function of the feed concentration. This phenomena seems to be related to the decreasing of the Donnan exclusion effect due to the solute higher diffusivity.

In Figure 6 it is shown the surfactant rejection as a function of the feed concentration for two tangential velocities: 0.2 and 0.7 m/s at 14 °C. It can be seen that with increasing the tangential flux the rejection becomes larger, mainly in the critical micellar region. This behavior should be related with the decay of free surfactant molecules close to the membrane surface. The increase of the tangential feed flux should improve the ability of the micelles to clean up this free molecules.

The maximum permeate flux and rejection obtained, 204 L/(m^2·h) and 99.5% respectively, are significantly higher than the results presented by Akay and Wakeman (*12*) for a similar system but using ultrafiltration. These authors report a permeate flux of 72 L/(m^2·h) for the ultrafiltration of a 200

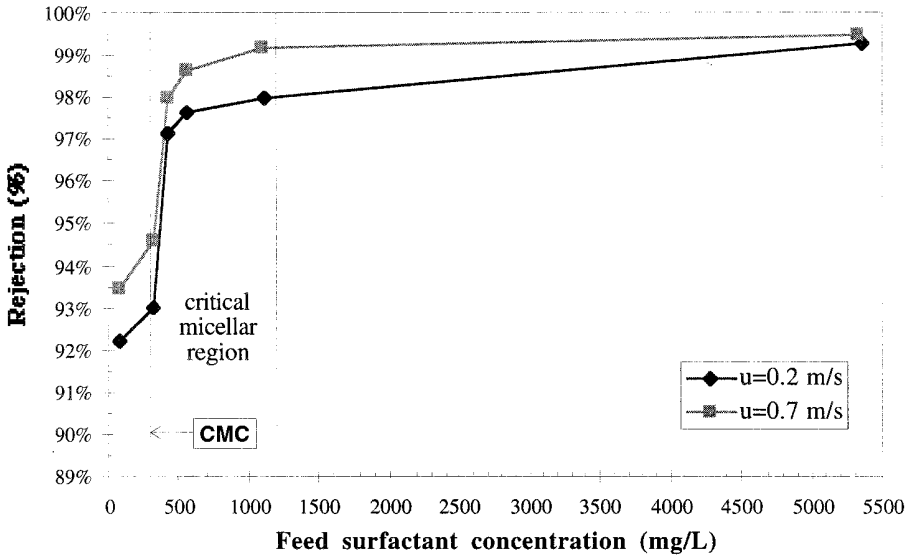

FIGURE 6. Rejection as a function of the feed surfactant concentration for two different cross-flow velocities, 0.2 and 0.7 m/s, at 14 °C.

mg/L anionic surfactant solution. They also report similar permeate fluxes for other ionic and nonionic surfactant solutions, with cmc lower than 200 mg/L.

Cabasso (*21*) studied the rejection of an anionic surfactant, the sodium dodecil-sulfate, on a ultrafiltration membrane of poly(dimethylphenilene oxide) which is positive charged. This author verified the rejection increased with the feed concentration, during the precritical micellar region and rapidly increased during the critical micellar region. After this region, the rejection leveled off for values close to 90%. This ultrafiltration system has a lower rejection than the nanofiltration system used in this work.

Taking into account the different kinds of the available surfactants and the multiple physicochemical interactions with the membranes, it is possible to criteriously choose from experimental work a pair surfactant/membrane for specific environmental applications involving separation processes.

The separation of substances by nanofiltration, however, is not restricted to the environmental area. The process selectivity and softness make it attractive for many biomedical and biotechnological applications, given the potential problems concerning the separation and purification of substances and biological constituents which are very specific and sensible. For instance, the use of asymmetric ultrafiltration membranes to fractionate solutions with different proteins has been studied (*22*).

We conclude from the present study that nanofiltration is a very promising technology for surfactant separation from water streams, having a higher performance than the traditionally used ultrafiltration. The permeate flux can be as much as three times larger and simultaneously have an equally higher rejection. However, the energy consumption for nanofiltration is higher.

The experimental results show that the nanofiltration pretreatment of industrial effluents containing the studied anionic surfactant up to a concentration of 1 g/L is a feasible process. This concentration level is a common situation in the chemical industry, the anionic surfactants, soaps, and detergents manufacturing, and in degreasing and cleaning operations in the automotive, aeronautic, and metal plating industries. Using nanofiltration, part of the surfactant can be recovered for reuse in the process and at the same time the organic load of the effluent, in terms of COD, is reduced, making the end-of-pipe treatment less expensive. The total oxidation of the sodium lauryl-ether-sulfate theoretically requires 1.93 g of O_2/g surfactant, which means that, in practice, the COD removal is twice that of the surfactant.

Other environmental applications of surfactants nanofiltration take advantage of the capacity of these substances to solubilize ionic compounds or organics, which cause changes in the surface characteristics of the membrane, as observed in ultrafiltration technologies previously described, e.g. MEUF. On the other hand, nanofiltration shows a higher selectivity in the separation of organics and mineral salts when compared with reverse osmosis and ultrafiltration.

Acknowledgments

The authors would like to thank Eng. José Guedes from Energest for providing the heat exchanger, Dr. Fiquet from Witco for supplying the technical information about the surfactant (used in this work), and Eng. José Garcia from Consorima for the surfactant sample. The collaboration of Mariana Simões from Alquímica laboratory, in the chemical analysis, is sincerely appreciated. The review of the medical terminology by Dr. Manuela Archer is also gratefully acknowledged.

Literature Cited

(1) *Wastewater Engineering: Treatment, Disposal and Reuse*; Metcalf & Eddy, Inc.: McGraw-Hill: New York, 1991; p 66.
(2) Mulder, M. In *Membrane Processes in Separation and Purification*; Crespo, J., Böddeker, K. W., Eds.; Kluwer Academic Publishers: Dordrecht, 1994; p 229.
(3) *Water Treatment Membrane Processes*; Odendaal, P., Wiesner, M., Mallevialle, J., Eds.; McGraw-Hill: New York, 1996.
(4) *Surfactant-based Separation Processes*; Scamehorn, J., Harwell, J., Eds.; Surfactant Science Series 28, Marcel Dekker: New York, 1989.
(5) Grieves, R.; Bhattacharyya, D.; Schomp, W.; Bewley, J. *AIChE J.* **1973**, *19*, 766.
(6) Wakeman, R. J.; Akay, G. *J. Membrane Sci.* **1995**, *106*, 57.
(7) Akay, G.; Wakeman, R. J. *Chem. Eng. Sci.* **1994**, *49*, 271.
(8) Akay, G.; Wakeman, R. J. *J. Membrane Sci.* **1994**, *88*, 177.
(9) Gadelle, F.; Koros, W. J.; Schechter, R. S. *Ind. Eng. Chem. Res.* **1996**, *35*, 3687.
(10) Yagi, H.; Uenishi, K.; Kushijima, H. *J. Ferment. and Bioeng.* **1993**, *76*, 306.
(11) Yildiz, E.; Pekdemir, T.; Keskinler, B.; Cakici, A.; Akay, G. *Trans. I. Chem. E* **1996**, *74*, Part A, 546.
(12) Akay, G.; Wakeman, R. J. *Chem. Eng. Res. Design* **1993**, *71*, Part A, 411.
(13) Dunn, R., O.; Scamehorn, J. F.; Christian, S. D. *Sep. Sci. Technol.* **1987**, *22*, 763.

(14) Raman, L.; Cheryan, M.; Rajagopalan, N. *Chem. Eng. Prog.* **1994**, *90*, 68.
(15) Markels, J.; Lynn, S.; Radke, C. *J. Membrane Sci.* **1994**, *86*, 241.
(16) Markels, J.; Lynn, S.; Radke, C. *AIChE J.* **1995**, *41*, 2058.
(17) Markels, J.; Lynn, S.; Radke, C. *Ind. Eng. Chem. Res.* **1995**, *34*, 2436.
(18) Miller, C.; Neogi, P. *Interfacial Phenomena: Equilibrium and Dynamic Effects*; Marcel Dekker: New York, 1985.
(19) *Standard Methods for the Examination of Water and Wastewater*; Greensberg, A. E., Clesceri, L. S., Eaton, A. D., Eds.; American Public Health Association: Washington, DC, 1992.
(20) Bird, R.; Stewart, W.; Lightfoot, E. *Transport Phenomena*; John Wiley & Sons: New York, 1960; p 29.
(21) Cabasso, I. In *Synthetic Membranes*; Turback, A. F., Ed.; ACS Symposium Series 154; American Chemical Society: Washington DC, 1981; Vol. 1.
(22) Opong, W.; Zydney, A. *AIChE J.* **1991**, *37*, 1497.

Received for review July 20, 1998. Revised manuscript received April 28, 1999. Accepted May 24, 1999.

ES980737C